Sensitivity to detector alignment

Maher Quraan

June 25, 2004

Data sets were analyzed using different alignment and geometry files to investigate the effects of chamber translational misalignments in the UV direction, rotational misalignments around the z-axis of the detector, and misalignments along the z-direction. The same set was used as a base set and a test set in order to reduce the statistical error and examine the systematic effects closely.

1 Effects of translational misalignments

A standard set was analyzed (set3anal6) with the plane UV positions randomly shifted by a $\sigma = 140\mu m$ (see posting by Dick Mischke 20-05-2004), and compared to a standard analysis of set3 (set3anal1). Both sets were analyzed with the same executable and all other settings were identical. Energy calibrations show a $13 \pm 7keV$ for the endpoint energy and a deterioration of the resolution to $81 \pm 2keV$ compared to $72 \pm 1keV$ for the standard set.

Figure 1 shows a comparison of the 1-dimensional normalized momentum and $\cos(\theta)$ histograms for the two cases. Figure 2 shows the difference between the normalized histograms of figure 1.

Below are the fitting results. The fiducial volume chosen is $20.0MeV/c < p < 50.0MeV/c$ and $0.50 < cos(\theta) < 0.85$.

Data: spectrumStat(fiducial_bins=2160, fiducial_entries=1.67327e+07, min_bin_entries=3462)
Base: spectrumStat(fiducial_bins=2160, fiducial_entries=1.67729e+07, min_bin_entries=3487)

$\chi 2 = 369$
$ndf = 2156$
$confLevel = 1$
$\rho = (0.09 \pm 2.1) \times 10^{-3}$
$\delta = (0.00 \pm 1.9) \times 10^{-3}$
$\xi = (0.2 \pm 2.4) \times 10^{-3}$
$\eta = (-6.4 \pm 117) \times 10^{-3}$

2 Effects of rotational misalignments

A standard set was analyzed (set3anal7) with the planes randomly rotated around the z-axis of the detector by $\sigma = 0.039\mu m$ (see posting by Dick Mischke 20-05-2004). This

corresponds to a translational misalignment of up to $\sim 100\mu m$ at the edges of the chamber, resulting in a systematic shift that progressively has a bigger effect on large angle tracks. The set was compared to a standard analysis of set3 (set3anal1). Both sets were analyzed with the same executable and all other settings were identical. Energy calibrations show no shift in the endpoint energy ($-3 \pm 6keV$) and no obvious deterioration of the endpoint resolution ($73 \pm 1keV$).

Figure 3 shows a comparison of the 1-dimensional normalized momentum and $\cos(\theta)$ histograms for the two cases. Figure 4 shows the difference between the normalized histograms of figure 3.

Below are the fitting results. The fiducial volume chosen is $20.0MeV/c < p < 50.0MeV/c$ and $0.50 < cos(\theta) < 0.85$.

Data: spectrumStat(fiducial_bins=2160, fiducial_entries=1.5695e+07, min_bin_entries=3232)
Base: spectrumStat(fiducial_bins=2160, fiducial_entries=1.67729e+07, min_bin_entries=3487)

$\chi 2 = 221$
$ndf = 2156$
$confLevel = 1$
$\rho = (1.2 \pm 2.2) \times 10^{-3}$
$\delta = (1.8 \pm 1.9) \times 10^{-3}$
$\xi = (2.8 \pm 2.5) \times 10^{-3}$
$\eta = (71 \pm 119) \times 10^{-3}$

3 Combined effects of translational and rotational misalignments

The same set was also analyzed (set3anal8) with the planes randomly shifted and randomly rotated around the z-axis of the detector using the same misalignments as above. The set was compared to a standard analysis of set3 (set3anal1). Both sets were analyzed with the same executable and all other settings were identical. Energy calibrations show a $-10 \pm 7keV$ for the endpoint energy and a deterioration of the resolution to $84 \pm 2keV$ compared to $72 \pm 1keV$ for the standard set.

Figure 5 shows a comparison of the 1-dimensional normalized momentum and $\cos(\theta)$ histograms for the two cases. Figure 6 shows the difference between the normalized histograms of figure 5.

Below are the fitting results. The fiducial volume chosen is $20.0MeV/c < p < 50.0MeV/c$ and $0.50 < cos(\theta) < 0.85$.

Data: spectrumStat(fiducial_bins=2160, fiducial_entries=1.67826e+07, min_bin_entries=3440)

Base: spectrumStat(fiducial_bins=2160, fiducial_entries=1.67729e+07, min_bin_entries=3487)

$\chi 2 = 379$
$ndf = 2156$
$confLevel = 1$
$\rho = (0.8 \pm 2.2) \times 10^{-3}$
$\delta = (1.1 \pm 1.9) \times 10^{-3}$
$\xi = (1.8 \pm 2.5) \times 10^{-3}$
$\eta = (38 \pm 119) \times 10^{-3}$

4 Effects of misalignment of the planes z-position

A standard set was analyzed (set2anal8) with the plane Z positions randomly shifted by $\sigma = 300\mu m$. Both sets were analyzed with the same executable, however, the field map file was different (bfld_map.00012 for set2anal8 vs bfld_map.00004 for set2anal6). Energy calibrations show a $16 \pm 6keV$ for the endpoint energy and a deterioration of the resolution to $83 \pm 2keV$ compared to $72 \pm 1keV$ for the standard set.

Figure 7 shows a comparison of the 1-dimensional normalized momentum and $\cos(\theta)$ histograms for the two cases. Figure 8 shows the difference between the normalized histograms of figure 7. Statistically significant structures are seen at low momenta (outside the fiducial region), and in the $\cos(\theta)$ distribution inside and outside the fiducial region. Although it is difficult to assert, the difference in the field map files might be the cause of these structures rather than the plane z-position randomization. An analysis of set2 with the same field map file has not been done, but might be a worthwhile exercises if time permits (perhaps more so to understand field map effects than z-position misalignments).

Below are the fitting results. The fiducial volume chosen is $20.0MeV/c < p < 50.0MeV/c$ and $0.50 < cos(\theta) < 0.85$.

Data: spectrumStat(fiducial_bins=2160, fiducial_entries=1.88069e+07, min_bin_entries=3831)
Base: spectrumStat(fiducial_bins=2160, fiducial_entries=1.86699e+07, min_bin_entries=3847)

$\chi 2 = 586$
$ndf = 2156$
$confLevel = 1$
$\rho = (1.0 \pm 2.0) \times 10^{-3}$
$\delta = (1.9 \pm 1.8) \times 10^{-3}$
$\xi = (2.7 \pm 2.3) \times 10^{-3}$
$\eta = (28 \pm 111) \times 10^{-3}$

5 Discussion and Conclusions

Plane translational misalignments by $\sigma = 140\mu m$ show a moderate $\sim 10keV$ deterioration in the endpoint energy resolution, and no statistically significant effect on the Michel parameters. This is not particularly surprising, since the randomization of the plane positions does not result in any systematic effects, but rather an overall smearing of the energy and angle as a result of a lower spatial resolution. The amount of deterioration in endpoint energy resolution corresponding to the misalignments applied give us a measure of the scale of correspondence between endpoint energy resolution and spatial resolution. Assuming an alignment accuracy of $10\mu m$, the amount of deterioration in spatial resolution does not account for the discrepancy with the Monte Carlo.

Plane rotational misalignments of over seven times the rotational alignment accuracy show a small deterioration of the endpoint energy resolution (if any), but bigger shifts (statistically significant?) on the Michel parameters (note that the data sets are correlated, and the errors shown above have not been scaled down to their appropriate values). The small deterioration in the endpoint resolution is consistent with the result for translational misalignments, since it only results in a UV shift of $\sim 50\mu m$ half way between the center and the edge of the detector. The rotational misalignments, despite being random, however, do result in systematic shifts, since they progressively effect large angle tracks more (the UV position shift is bigger for bigger radii).

The combined translational and rotational misalignments show results that are consistent with the separate translational and rotational misalignments.

Misalignments along the z-direction by $\sigma = 300\mu m$ show a similar deterioration of the endpoint energy resolution. While the deterioration of the endpoint energy resolution is not surprising, the amount of deterioration (about $10keV$) corresponding to a $300\mu m$ randomization of the plane z-position is small compared to the plane z-position construction accuracy. Misalignments in the z-direction, therefore, cannot account for the discrepancy between data and Monte Carlo. The fitting results reflect deviations that maybe statistically significant (once again the errors are not scaled to account for correlations). Whether this is due to the field map being different or the z-position randomization is hard to discern. If these deviations (assuming they are not simply statistical fluctuations) are entirely due to z-position misalignments, they are still small enough once they are scaled down to the appropriate values (by a factor of ~ 10).

Since the final table requires an estimate of the misalignment systematic, and since these are not entirely uncorrelated (for example rotational and translational misalignments are correlated), it is perhaps best to analyze a set with all three misalignments combined (now that we understand the effect of each independently). The exaggeration factor for each misalignment effect has to be the same, however, to allow scaling down the results appropriately.

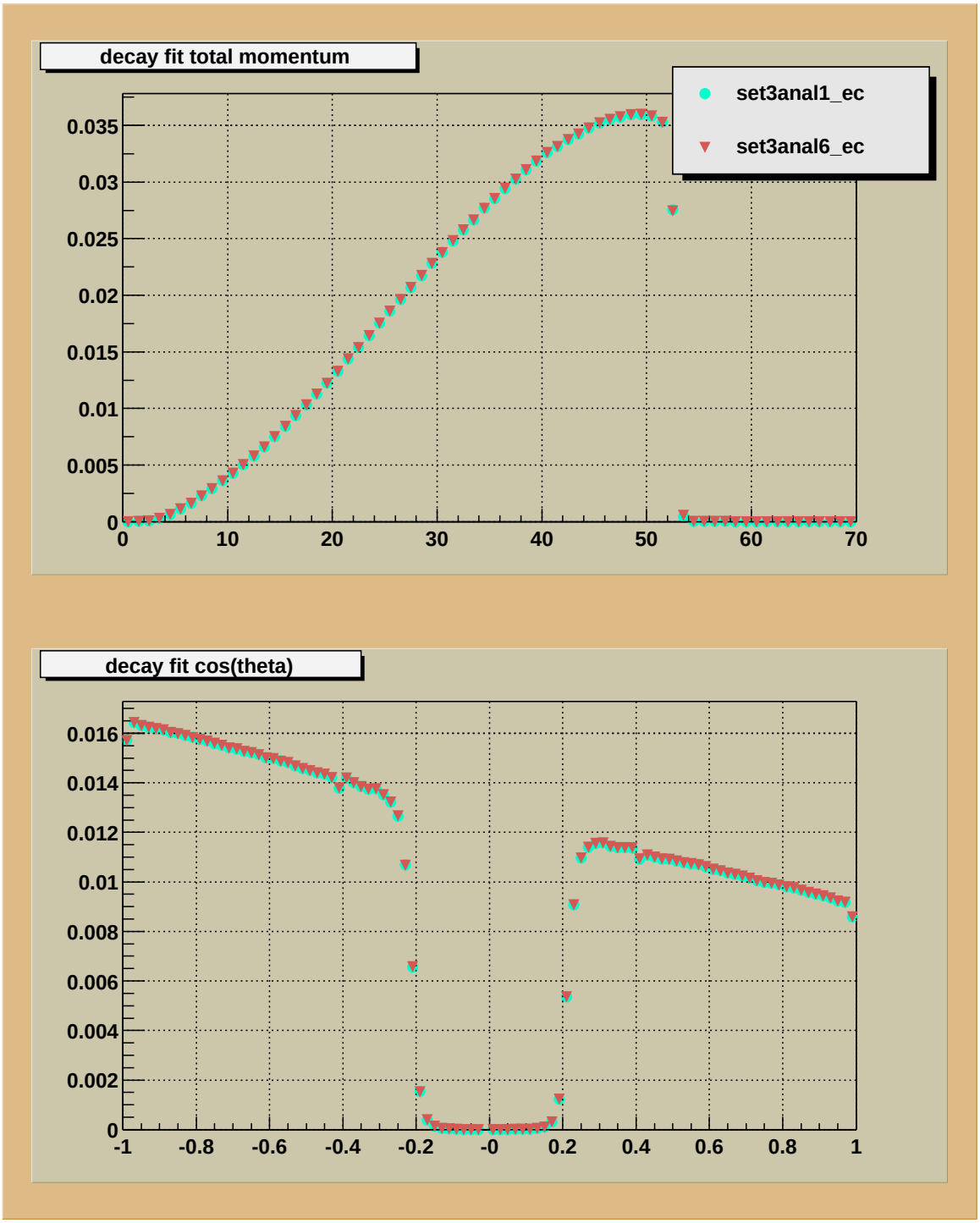

Figure 1: Momentum (top) and cos(θ) (bottom) distributions for the analysis of set3 using nominal plane positions in one analysis and randomly shifted UV plane positions in the second.

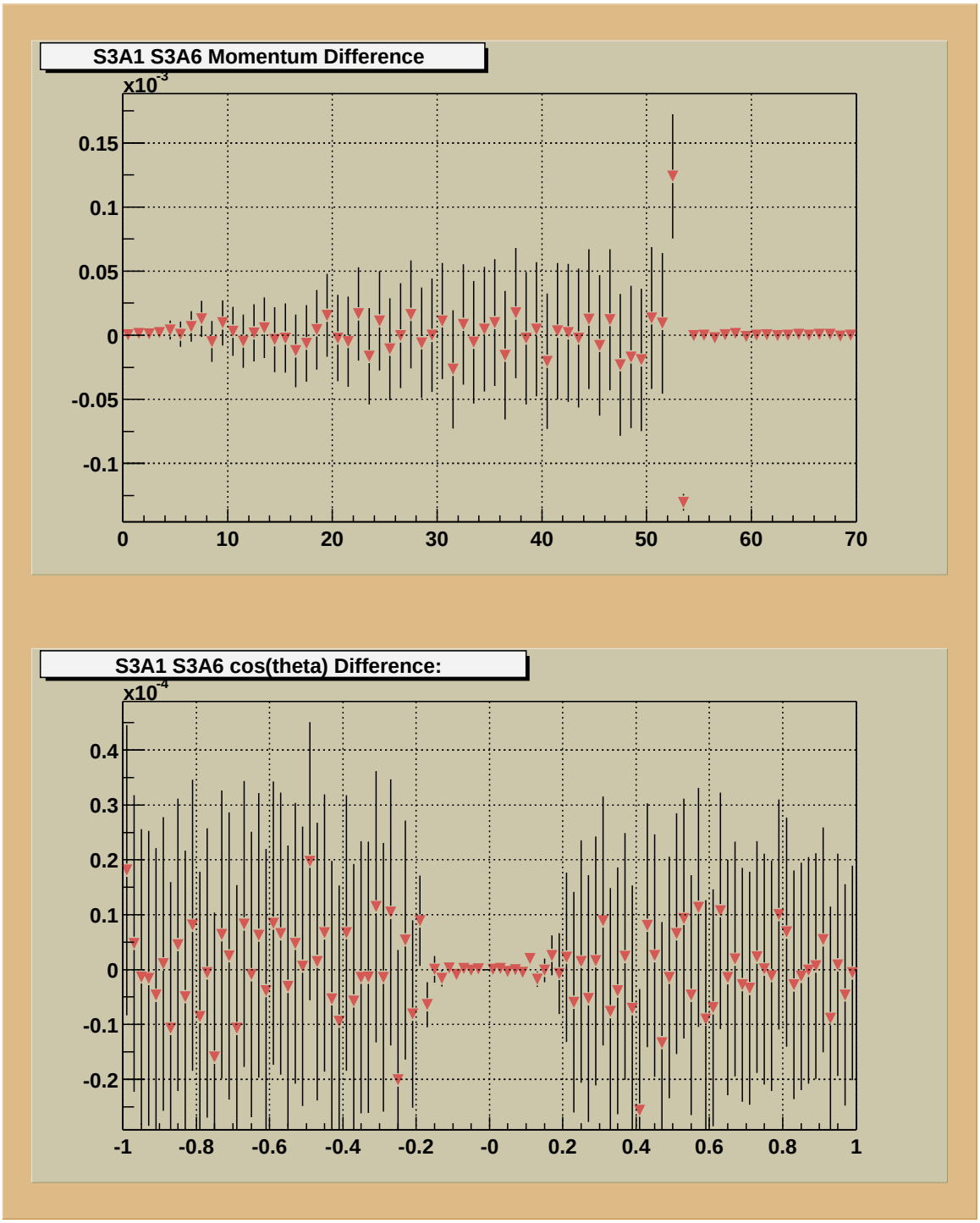

Figure 2: Momentum difference (top) and cos(θ) difference (bottom) for the analysis of set3 using nominal plane positions in one analysis and randomly shifted UV plane positions in the second.

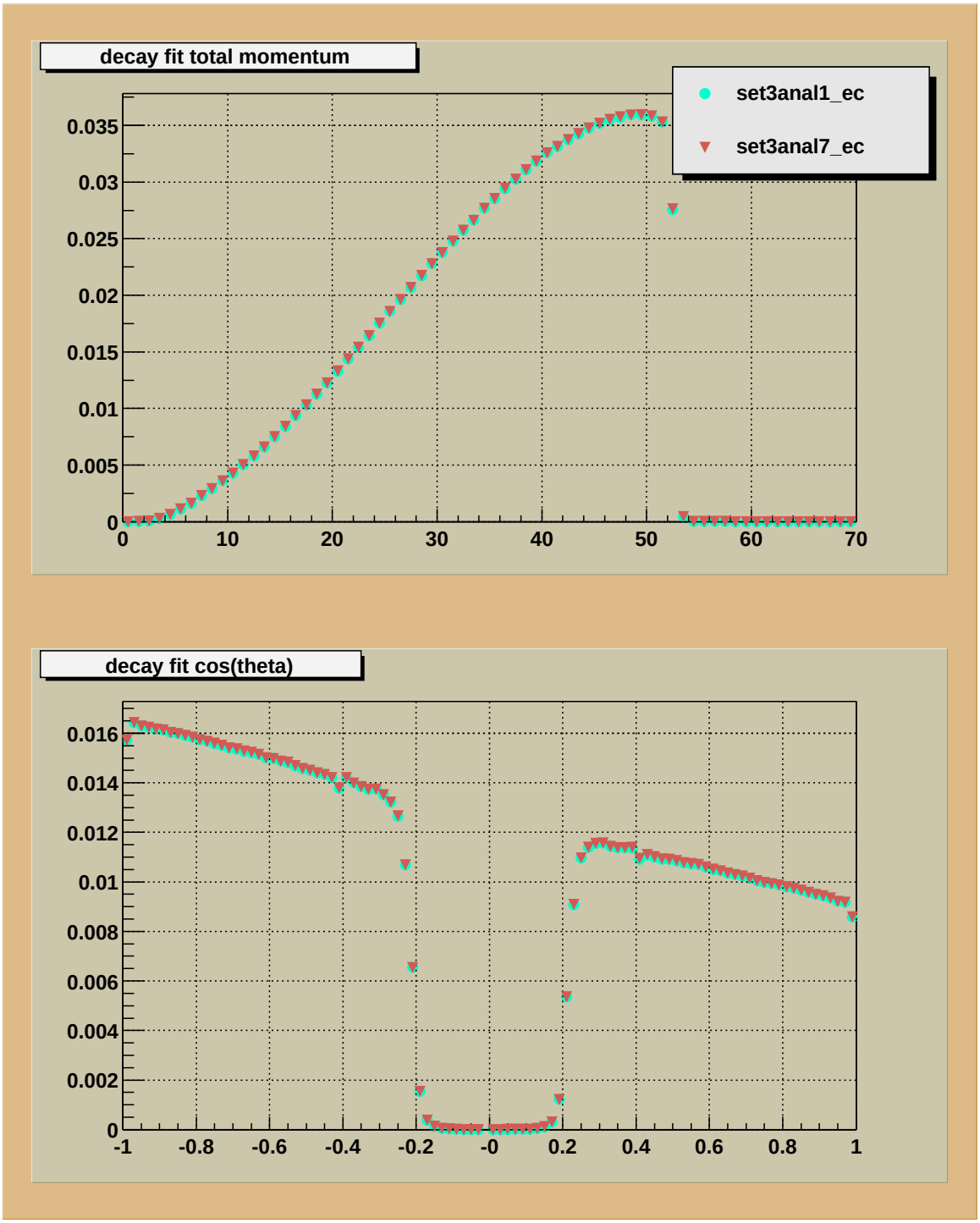

Figure 3: Momentum (top) and cos(θ) (bottom) distributions for the analysis of set3 using nominal plane positions in one analysis and randomly rotated plane positions in the second.

Figure 4: Momentum difference (top) and cos(θ) difference (bottom) distributions for the analysis of set3 using nominal plane positions in one analysis and randomly rotated plane positions in the second.

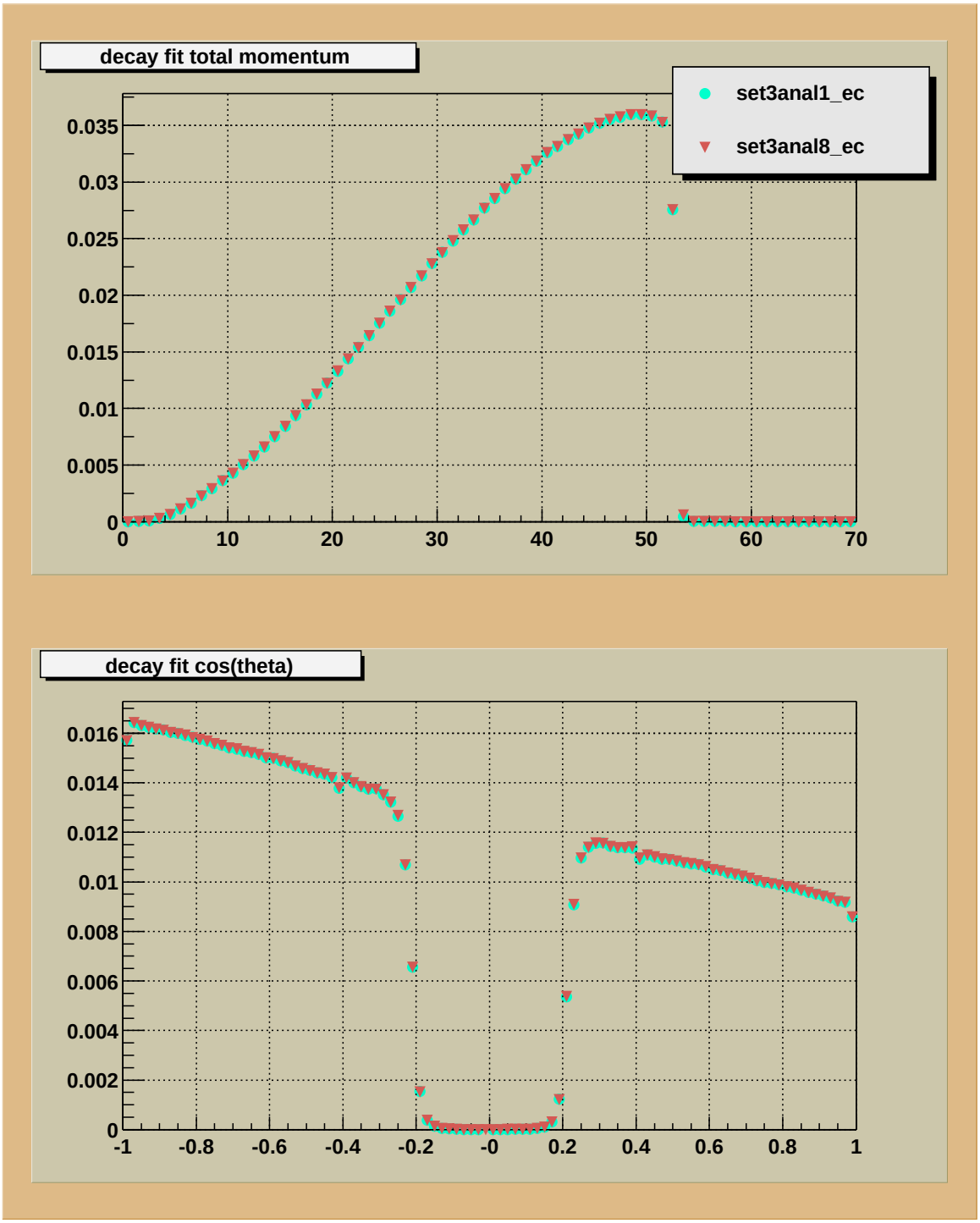

Figure 5: Momentum (top) and cos(θ) (bottom) distributions for the analysis of set3 using nominal plane positions in one analysis and randomly shifted and rotated plane positions in the second.

Figure 6: Momentum difference (top) and cos(θ) difference (bottom) distributions for the analysis of set3 using nominal plane positions in one analysis and randomly shifted and rotated plane positions in the second.

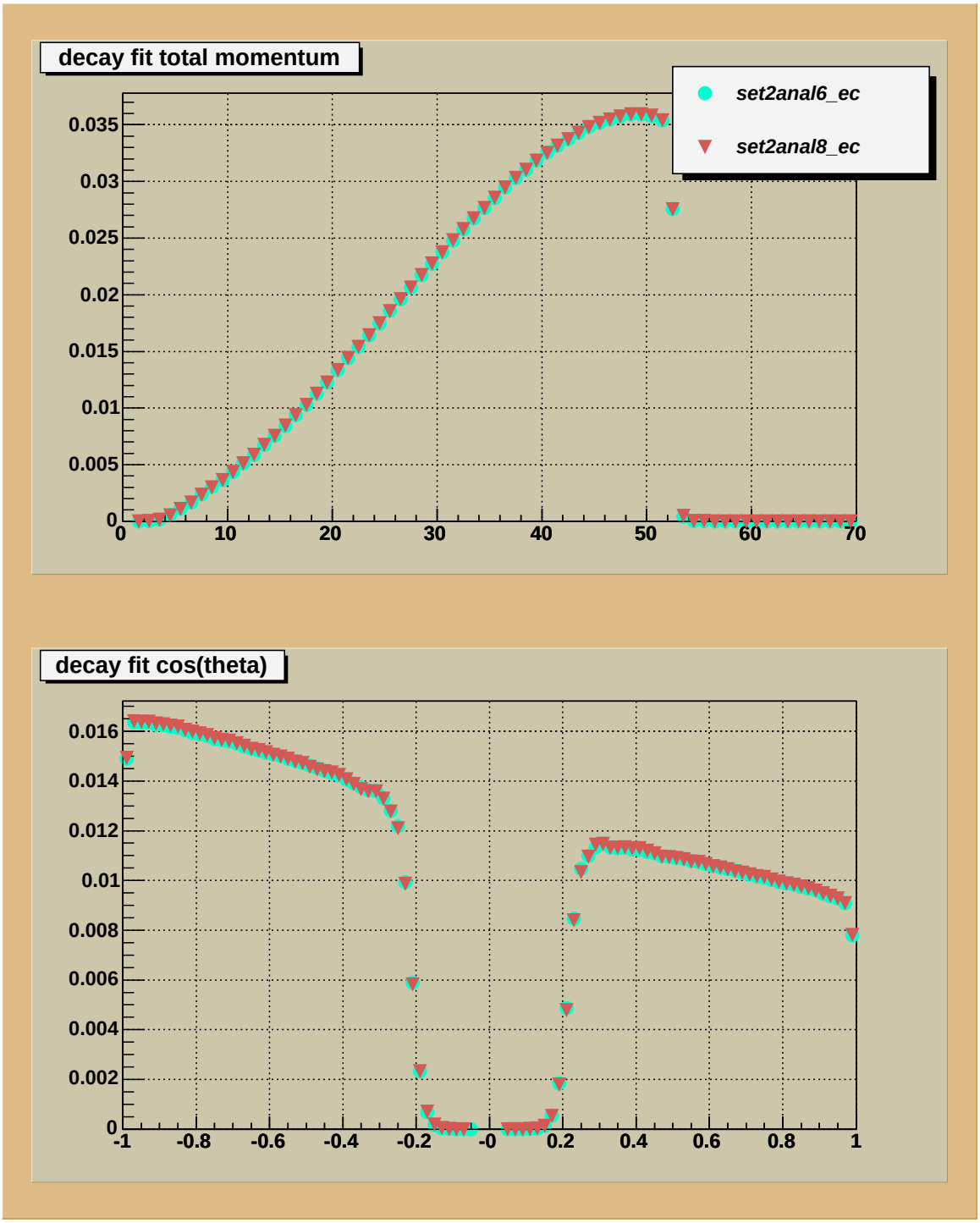

Figure 7: Momentum (top) and cos(θ) (bottom) distributions for the analysis of set3 using nominal plane positions in one analysis and randomly shifted z-positions in the second.

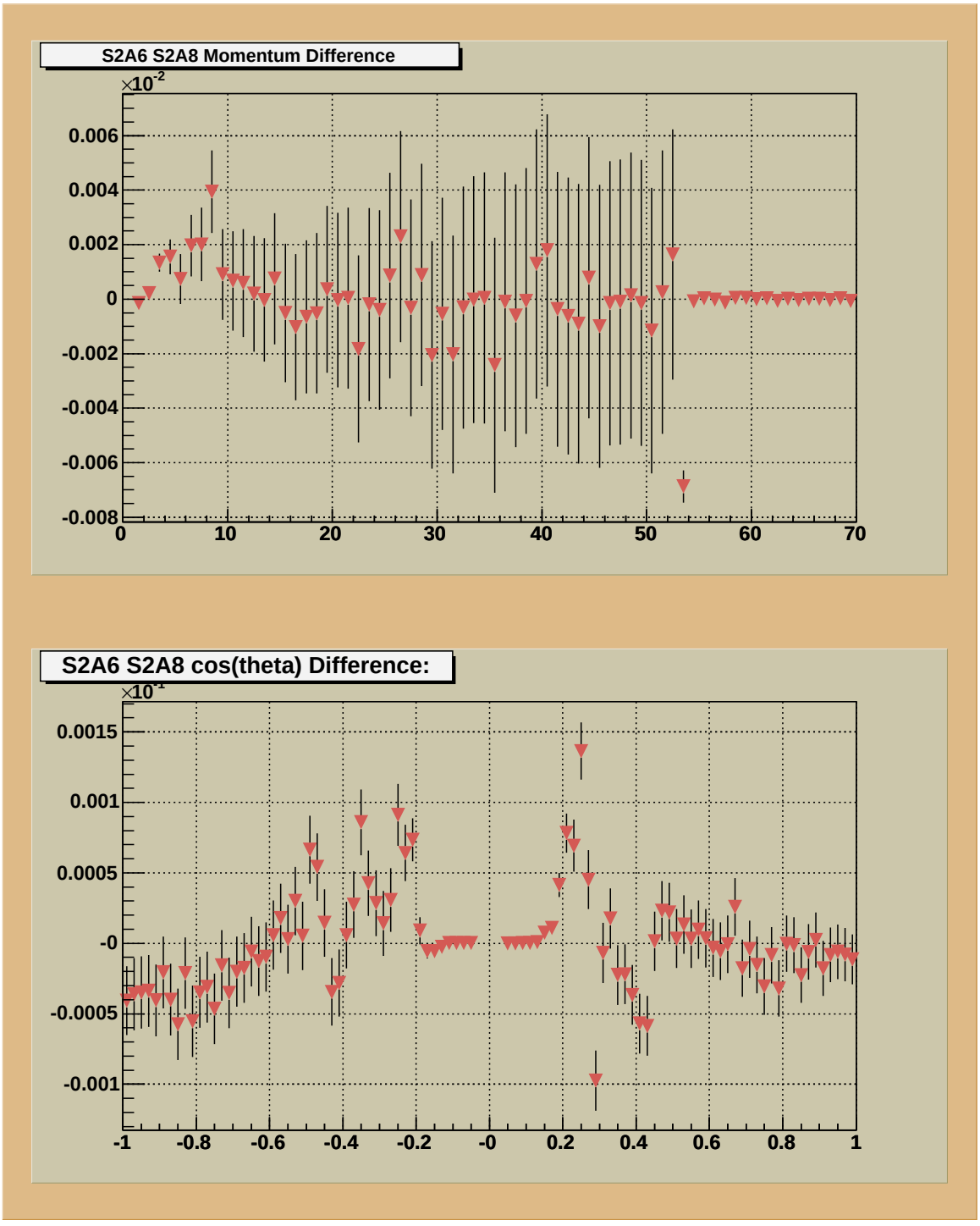

Figure 8: Momentum difference (top) and cos(θ) difference (bottom) for the analysis of set3 using nominal plane positions in one analysis and randomly shifted z-positions in the second.